



CHORUS

This is the accepted manuscript made available via CHORUS. The article has been published as:

Surface Hydration Amplifies Single-Well Protein Atom Diffusion Propagating into the Macromolecular Core

Liang Hong, Xiaolin Cheng, Dennis C. Glass, and Jeremy C. Smith

Phys. Rev. Lett. **108**, 238102 — Published 5 June 2012

DOI: [10.1103/PhysRevLett.108.238102](https://doi.org/10.1103/PhysRevLett.108.238102)

**Surface hydration amplifies single-well protein atom diffusion propagating
into the macromolecular core**

Liang Hong,^{1,2} Xiaolin Cheng,^{1,2} Dennis C. Glass,¹ and Jeremy C. Smith^{1,2}

¹ *UT/ORNL Center for Molecular Biophysics, Oak Ridge National Laboratory
P. O. Box 2008, Oak Ridge, TN 37831, USA*

² *Department of Biochemistry and Cellular and Molecular Biology, University of
Tennessee, M407 Walters Life Sciences, 1414 Cumberland Avenue, Knoxville, TN
37996, USA*

Abstract

The effect of surface hydration water on internal protein motions is of fundamental interest in molecular biophysics. Here, by decomposing the *ps-ns* atomic motions in molecular dynamics simulations of lysozyme at different hydration levels into three components - localized single-well diffusion, methyl group rotation and non-methyl jumps - we show that the effect of surface hydration is mainly to increase the volume of the localized single-well diffusion. These diffusive motions are coupled in such a way that the hydration effect propagates from the protein surface into the dry core.

PACS: 87.15.H-, 87.15.ap, 87.64.Bx, 87.14.E-

*Author to whom correspondence should be addressed: smithjc@ornl.gov

Internal motions in globular proteins are crucial for their function [1, 2] and depend significantly on surface hydration [3]. Most protein studies have shown that at physiological temperatures hydration enhances anharmonic motions of atoms in protein molecules [3-6]. Intriguing questions have arisen as to whether the hydration effect is mainly local and limited to the protein surface, or rather is global, propagating into the functional core, and if the latter, what the mechanism of the propagation might be. NMR and fluorescence anisotropy experiments have provided some evidence that hydration indeed significantly promotes *ps-ns* atomic motions in the protein interior [7-9]. However, proteins exhibit a wide variety of diffusive and vibrational dynamics on these time scales [4, 6, 10, 11], and most experimental techniques provide only averaged information, rendering difficult the characterization of the microscopic nature of the hydration-promoted atomic motions and of the mechanisms by which the dynamical hydration effects may propagate from the surface into the core. This information can, in principle, be provided by molecular dynamics (MD) simulations.

Most MD studies have hitherto focused on the effect of hydration on accelerating conformational transitions in proteins [12-16], such as those between torsional rotameric states [13, 14]. However, intuitively, local surface dihedral transitions, such as those of side chains, would not necessarily be expected to collectively propagate into the protein core. The present work combines neutron scattering and MD simulation to show that a major hydration effect on protein dynamics on the *ps* to *ns* time scales is to enlarge the volume accessible to single-

well diffusion of individual protein atoms, and that strong coupling between these single-atom diffusive motions propagates the effect from the protein surface into its interior.

Lysozyme powder simulations were performed at three hydration levels (h): 0.05, 0.3 and 0.5 grams of water per gram of protein. $h = 0.05$ refers to “dry” powder, while $h = 0.5$ corresponds to the fully hydrated case [3]. Details of the simulation systems and MD protocol are provided in the Supplemental Material [17].

Incoherent neutron scattering has been widely applied to study atomic motions in proteins [5, 6, 10, 18-22], as neutrons directly probe fluctuations in nuclear positions. Here, the incoherent neutron scattering spectra were computed from the MD trajectories using in-house software. Details are provided in Ref. [10]. It is informative to present the neutron scattering spectra as the imaginary part of the dynamic susceptibility, $\chi''(q, \nu) \propto \frac{S(q, \nu)}{n_B(\nu)}$, where $n_B(\nu)$ is the Bose occupation number $n_B(\nu) = (\exp(h\nu/kT) - 1)^{-1}$, q is the scattering wavevector and $S(q, \nu)$ is the dynamic structure factor, as relaxation processes on different time scales appear as distinct peaks in χ'' with associated relaxation times $\tau = 1/2\pi\nu$ [6, 10]. In Fig. 1, we compared χ'' at different hydration levels derived from MD simulation with the corresponding experimental data, which have been obtained by combining results from three instruments [6, 17, 23]. The coefficient of determination (R^2) as defined

in Ref. [17], i.e., a standard evaluator to quantify the matching between two sets of data, is found to be close to 1 for both the hydrated ($h = 0.3$, $R^2 = 0.85$) and the dry ($h = 0.05$, $R^2 = 0.95$) samples, indicating that the simulation-derived spectrum agrees quantitatively with the experimental result in a wide frequency window. χ'' shows a broad peak, the so-called “main” relaxation peak [10], covering the ~ 1 to 100 GHz frequency range, corresponding to atomic motions on the time scales of a few to hundreds of ps . As dynamics on these time scales has attracted much interest [1, 3, 4, 6, 10, 11, 18-22], in what follows the discussion focuses on this main relaxation peak.

To understand the microscopic details of the protein atomic motions underlying the main relaxation peak, the coordinates of each hydrogen atom at every 1 ps in a 10 ns trajectory were projected onto scatter plots [10], examples of which are presented in Fig. S1. Some scatter plots exhibit a single cluster (e.g., Fig. S1a), corresponding to diffusion in a localized region, whereas others possess several clusters (e.g., Figs. S1b and c), corresponding to a combined motion of localized, intra-cluster diffusion and jumps between clusters. We name hydrogen atoms undergoing only localized diffusion (e.g., Fig. S1a) as “locally-diffusing” atoms. The “jumps between clusters” can be further differentiated into methyl group rotations (e.g., Fig. S1c) and non-methyl jumps (e.g., Fig. S1b), and these have been found to exhibit distinct neutron spectra [10]. For simplicity, the non-methyl jumps are named as “jumps”. As a result, the protein atomic motions on the

ps - *ns* time scales involve three simple components: localized diffusion, methyl group rotations and jumps [10]. The neutron spectra of these components can be calculated separately and details are given in Ref. [17]. An example at $h = 0.3$ is presented in Fig. S1d. The spectrum of the localized diffusion (χ''_{ld}) is quite flat in the frequency window ~ 1 - 100 GHz, whereas the methyl group rotations (χ''_{me}) present a noticeable peak located around 10 GHz and the signal of the jumps (χ''_{jump}) is seen mainly below 10 GHz.

As is evident in Fig. 2a, the amplitude of the main relaxation peak is elevated significantly with h , i.e., the mobility of the protein atoms is enhanced by hydration [24]. The neutron scattering spectra at each h , decomposed as described in Ref. [17], are presented in Figs. 2b-d. Whereas the amplitude of χ''_{ld} increases strongly with h , χ''_{jump} exhibits only a weak hydration dependence and χ''_{me} is effectively hydration independent. The latter finding is consistent with experimental neutron scattering data showing that the low-temperature anharmonic onset of the methyl group rotation at ~ 100 K is hydration independent [6, 18], and also agrees with the simulation work indicating that the rotational mobility of methyl groups is independent of solvent exposure [25].

Quantitative analysis of the neutron scattering spectra (see Fig. S2 and the corresponding text in Ref. [17]) shows that the localized diffusion accounts for $\sim 80\%$ of the hydration-induced increase of the amplitude of the main relaxation peak of the protein, whereas “jumps” play only a secondary role ($\leq 20\%$) and the

methyl group rotations contribute negligibly. Hence, majority of the hydration-induced change in the protein dynamics on the ps to ns time scales results from the localized diffusion.

The drastic increase of the neutron scattering intensity of the localized diffusion (Figs. 2c, S2a and b) indicates that the diffusional amplitude is enlarged by hydration [24]. This is quantified in Fig. 3a, in which the distribution of the motional amplitudes of the locally-diffusing hydrogen atoms, as characterized by R_g (the radius of gyration of the scatter plots), is shown to shift significantly to higher values with h . This shift occurs not only on the protein surface but also in the core (Figs. S3a and b), consistent with observations in NMR and fluorescence anisotropy experiments that hydration enhances the mobility of residues both on the protein surface and in its interior [7, 8]. (A protein hydrogen atom was defined as a surface atom if it is in close contact with water molecules when the protein is fully hydrated, and otherwise was assigned to the core, see details in Ref. [17].) Table SII [17] presents the average motional amplitudes of the locally-diffusing atoms, i.e., \bar{R}_g , at different h . The ratio of $\frac{\bar{R}_g(h)}{\bar{R}_g(0.05)}$ for the protein surface is only slightly larger than that for the core, indicating that majority of hydration effect indeed propagates into the protein interior.

The change of atomic motions may be associated with a variation of the underlying potential of mean force (PMF) [1, 12, 26]. Here the PMF of each hydrogen atom was calculated using $W(r) = -RT \ln P(r)$ [26] where R is the gas

constant, $P(r)$ is the probability distribution of the atomic position in the scatter plot, and r is the distance from the center. $W(r)$ thus obtained is a 1D projection of the 3D PMF of a given atom. An example, calculated for a typical locally-diffusing hydrogen atom, is displayed in Fig. S4, indicating that the “localized diffusion” corresponds to an atomic motion confined in a single potential well. In contrast, methyl group rotation and jumps involve inter-well transitions. As seen in Figs. 2d, S2a and b, the neutron scattering signal arising from jumps is also boosted by increasing h . Table SIII [17] presents the number of hydrogen atoms conducting jumps (N_{jump}) and the average jumping distance (D_{jump}) at different hydration levels. N_{jump} increases significantly with h whereas D_{jump} remains approximately constant. Hence, hydration also facilitates inter-well transitions, as previously found [4, 12-15].

As the localized diffusion accounts for most of the observed hydration-induced change in the protein dynamics, in what follows we focus on the hydration dependence of $W(r)$ of locally-diffusing hydration atoms. The example in Fig. S4 shows that $W(r)$ becomes wider with h . For quantitative comparison, r_w , the width of $W(r)$, is defined here as the value of r at which $W(r) = 10kJ/mol$, corresponding roughly to the barrier of the methyl group rotations [10]. As seen in Fig. 3b, the distribution of r_w shifts significantly to larger values with h , i.e., hydration widens the single-atom potential of mean force. Broadening of the PMF at a given temperature can be interpreted as reduction of the effective force constant in the harmonic approximation. This is broadly consistent with the concept that hydration

reduces the internal “resilience” of proteins, as derived from neutron scattering studies on the temperature dependence of the mean-square atomic displacement (MSD) [22], and is also in agreement with the measurement of the sound velocity of lysozyme crystals showing that the associated elastic constant decreases with hydration [27]. Comparison of the values of $\frac{\bar{r}_w(h)}{\bar{r}_w(0.05)}$ (Table SII) for the surface and core atoms reveals that both exhibit pronounced hydration-induced widening of $W(r)$, albeit the variation of the former is slightly more significant, in agreement with the above analysis of the diffusional amplitude.

Fig. 3 and Table SII demonstrate that hydration broadens the potential of mean force of protein atoms, facilitating the diffusion of atoms both on the protein surface and in the core. The question thus arises as to how the hydration effect propagates into the protein interior. To address this, principal component analysis (PCA) was carried out on a trajectory, labeled as T_{LD} , from which the methyl group rotation and jumps are removed such that only the localized diffusion remains intact, thus preserving the majority of the hydration-induced change in the protein dynamics (Details are given in Ref. [17]).

The resulting PCA modes were arranged in descending order of the associated mean square fluctuation of atomic position (MSF). The cumulative contribution of the first n PCA modes to the localized diffusion of all protein atoms at a given hydration level is then given by,

$$\gamma_n(h) = \frac{\sum_{i=1}^n \langle u^2 \rangle_i}{\langle u^2 \rangle}, \quad (1)$$

where $\langle u^2 \rangle_i$ is the MSF of the i th PCA mode, and $\langle u^2 \rangle$ is the total MSF of the atoms in Trajectory T_{LD} . Fig. 4a shows that the low-index PCA modes contribute much more significantly than the high-index ones. For example, the first 25 modes at $h = 0.3$, i.e., the first 1% of the total modes, account for $\sim 40\%$ of $\langle u^2 \rangle$.

Fig. 4b displays the number of atoms participating significantly in each PCA mode (the definition of “participating significantly” is given in Ref. [17]) and demonstrates that the low-index PCA modes are highly collective motions. Furthermore, the inset of Fig. 4b reveals that these collective modes involve both surface and core atoms, i.e., they run through the whole protein molecule.

Together Figs. 4a and b demonstrate that the localized diffusion of individual protein atoms is strongly coupled through the whole protein molecule, thus enabling the hydration effect on atomic diffusion to propagate from the protein surface into its interior.

The potential of mean force, or namely the effective free energy, along each PCA mode is given by $\mu_i(q_i) = -RT \ln G_i(q_i)$ [28], where $G_i(q_i)$ is the probability distribution along the i th mode and q_i is the corresponding reaction coordinate. Fig. S6 [17] presents $\mu_i(q_i)$ of the first nine modes at different h . Clearly, $\mu_i(q_i)$ becomes wider with increasing h . Hence, the global protein energy

landscape, in terms of the effective free energy along the low-index PCA modes, is broadened or softened by hydration. This is consistent with the widening of the energy landscapes of individual atoms (Fig. 3b), as the associated atomic fluctuations, i.e., the locally diffusive motions, are highly collective.

The effect of hydration on protein dynamics has been extensively studied in the past, but the focus has been on the promotion of conformational transitions [4, 12-15]. This effect is confirmed in the present work by the result that the number of protein atoms undergoing inter-well jumps is increased upon hydration. However, here we provide evidence for a new physical picture in which, on the *ps* to *ns* time scales, the effect of hydration is mainly to enlarge the volume accessible to localized diffusion of protein atoms in single wells, and that this effect propagates significantly into protein interior via strong coupling between these diffusive motions, thus softening the whole protein molecule.

Analysis of MD simulation results of another very different protein, green fluorescent protein (GFP), presented in the Supplemental Material [17] results in the same conclusions as for lysozyme. As GFP and lysozyme greatly differ in size, shape and secondary structural composition, it is likely that the hydration effect on protein dynamics revealed in the present work will be valid for many or most folded globular proteins.

Acknowledgment

We thank Dr. Nikolai Smolin for producing part of the codes for analyzing the MD trajectories, Dr. Alexi P. Sokolov for providing the neutron scattering data in a convenient form, and Dr. E. Mamontov's for analyzing the BASIS data. We acknowledge funding from NSF grant [MCB-0842871].

References

- [1] H. Frauenfelder, S. G. Sligar, and P. G. Wolynes, *Science* **254**, 1598 (1991).
- [2] K. A. Henzler-Wildman *et al.*, *Nature* **450**, 7171 (2007).
- [3] J. A. Rupley, and G. Careri, *Adv. Protein Chem.* **41**, 37 (1991).
- [4] W. Doster and M. Settles, *Biochim. Biophys. Act.* **1749**, 173 (2005).
- [5] M. Ferrand *et al.*, *Proc. Natl. Acad. Sci. U.S.A.* **90**, 9668 (1993).
- [6] J. H. Roh *et al.*, *Biophys. J.* **91**, 2573 (2006).
- [7] A. Tamura *et al.*, *Protein. Sci.* **5**, 127 (1996).
- [8] G. Careri, and E. Gratton, in *The Fluctuating Enzyme*, edited by G. R. Welch, John Wiley & Sons, New York, p. 239 (1986).
- [9] J. M. Zanotti, M. C. Bellissent-Funel, and J. Parello, *Biophys. J.* **76**, 2390 (1999).
- [10] L. Hong *et al.*, *Phys. Rev. Lett.* **107**, 148102 (2011).
- [11] E. Kussell, and E. I. Shakhnovich, *Phys. Rev. Lett.* **89**, 168101 (2002).
- [12] A. Kitao, F. Hirata, and N. Go, *Chem. Phys.* **158**, 447 (1991).
- [13] P. J. Steinbach, and B. R. Brooks, *Proc. Natl. Acad. Sci. U.S.A.* **90**, 9135 (1993).
- [14] B. M. Pettitt, and M. Karplus, *Chem. Phys. Lett.* **121**, 194 (1985).
- [15] K. Hinsén, and G. R. Kneller, *Proteins* **70**, 1235 (2008).
- [16] R. M. Daniel *et al.*, *Annu. Rev. Biophys. Biomol. Struct.* **32**, 69 (2003).
- [17] See Supplemental Material.
- [18] G. Schiro *et al.*, *Phys. Chem. Chem. Phys.* **12**, 10215 (2010).

- [19] J. Fitter *et al.*, Proc. Natl. Acad. Sci. U.S.A. **93**, 7600 (1996).
- [20] W. Doster, S. Cusack, and W. Petry, Nature **337**, 754 (1989).
- [21] S. H. Chen *et al.*, Proc. Natl. Acad. Sci. U.S.A. **103**, 9012 (2006).
- [22] K. Wood *et al.*, Chem. Phys. **345**, 305 (2008).
- [23] S. Khodadadi *et al.*, J. Chem. Phys. **128**, 195106 (2008).
- [24] M. Bee, Quasielastic neutron scattering, Adam Hilger, Philadelphia (1988).
- [25] M. Krishnan, V. Kurkal-Siebert, and J. C. Smith, J. Phys. Chem. B **112**, 5522 (2008).
- [26] A. H. Zewail *et al.*, Proc. Natl. Acad. Sci. U.S.A. **104**, 17261 (2007).
- [27] S. Speziale *et al.*, Biophys. J. **85**, 3202 (2003).
- [28] A. L. Tournier, and J. C. Smith, Phys. Rev. Lett. **91**, 208106 (2003).

Figure Caption

Fig. 1 (color online). Hydration dependence of the susceptibility spectra of lysozyme ($q = 1 \text{ \AA}^{-1}$) at 295K obtained from neutron scattering experiments on the NIST high-flux backscattering spectrometer (HFBS, triangles), the ORNL SNS back-scattering spectrometer (BASIS, spheres), and the NIST disk-chopper time-of-flight spectrometer (TOF, squares) [6, 17, 23] and from MD simulation (thick solid line). To improve the statistics, the experimental spectra were summed over the q range from 0.3 to 1.7 \AA^{-1} with an average $q = 1 \text{ \AA}^{-1}$. As the statistics of the simulation-derived spectra are much better, only data at $q = 1 \text{ \AA}^{-1}$ are presented. For ease of comparison of the two sets of spectra, the experimental data on the y axis have been rescaled by a same constant. Experimental details can be found in Ref. [17].

Fig. 2 (color online). Susceptibility spectra of lysozyme at different hydration levels, h : (a) total protein dynamics (χ''), (b) methyl group rotation (χ''_{me}), (c) localized diffusion (χ''_{ld}) and (d) jumps (χ''_{jump}) at $q = 1 \text{ \AA}^{-1}$.

Fig. 3 (color online). Hydration dependence of the distribution of (a) R_g of the scatter plots and (b) r_w of the locally-diffusing hydrogen atoms, where $W(r_w)$ is 10 kJ/mol . The choice of the value of $W(r_w)$ is not crucial, and variation within reason does not alter the conclusions (see Fig. S5 in Ref. [17]).

Fig. 4 (color online). (a) Cumulative contribution of PCA modes to the localized diffusion of protein atoms, $\gamma_n(h)$ calculated using Eq. (1). (b) Number of significantly-participating (S.P.) atoms in each PCA mode. The inset presents the percentage of surface atoms in the significantly-participating atoms for each PCA mode at $h = 0.3$.

Fig. 1

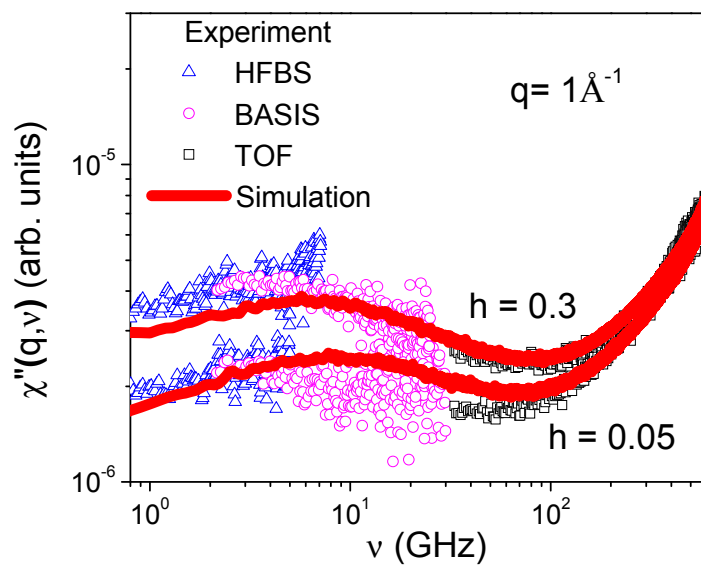


Fig. 2

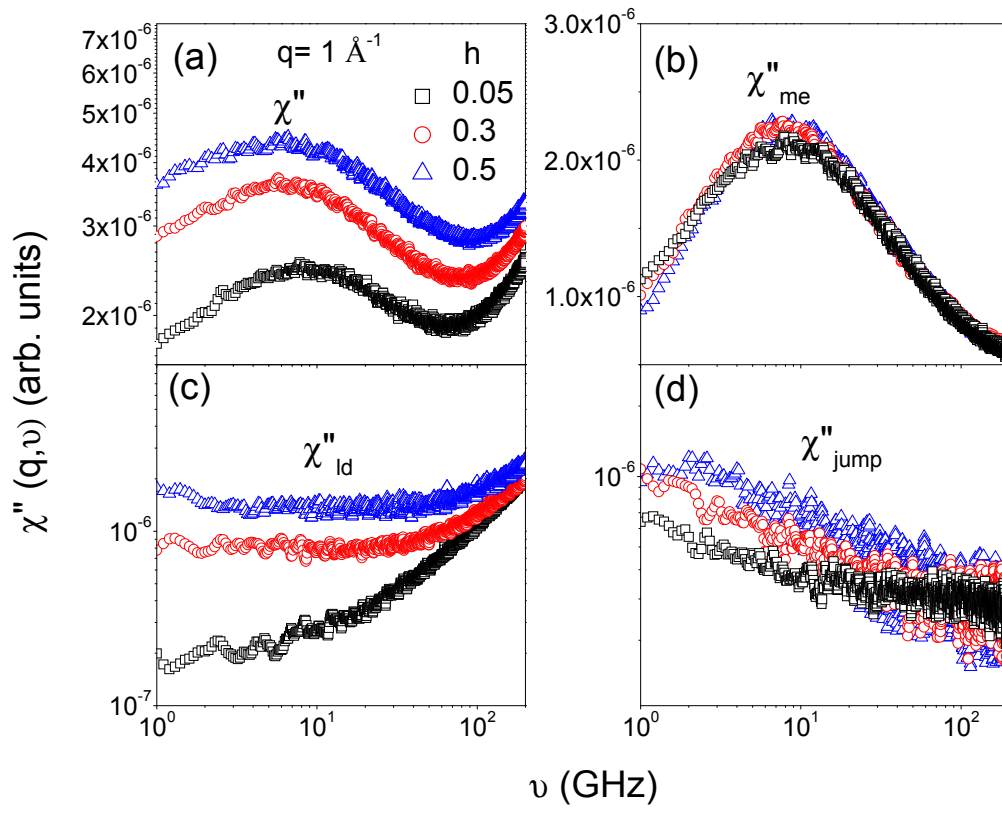


Fig. 3

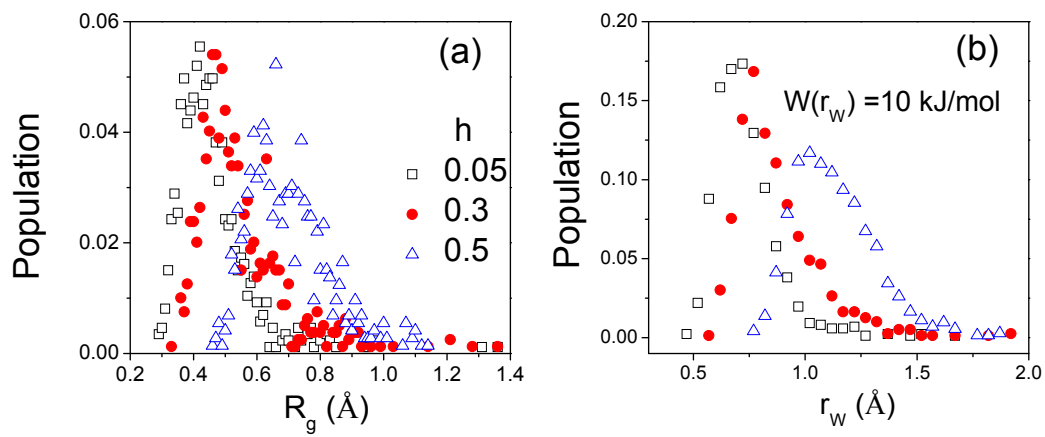


Fig. 4

